 DOI: 10.1002/masy.200750353

Model Supported Morphology Control of Electrospray Deposited Poly(vinylidene fluoride) Film

Ivo B. Rietveld,[*1,2] *Kei Kobayashi,*[1,2] *Hirofumi Yamada,*[1] *Kazumi Matsushige*[1,2]

Summary: Preparation of polymer films with electrospray deposition has been investigated. Morphologies of poly(vinylidene fluoride), prepared under a range of different conditions, have been imaged with AFM. To generalize the conditions under which a particular morphology appears, a model has been used. The model incorporates the parameters that determine droplet size and droplet evaporation in the electrospray deposition process. With the model, film morphology has been shown to depend on the droplet volume at impact, available surface area on the substrate and rate of solvent evaporation from the film. With this information, the model can predict the film morphology under many different spray conditions. This has been demonstrated by determining and predicting the conditions under which PVDF displays the smoothest films.

Keywords: AFM; electrohydrodynamic atomization; film roughness; fluoropolymers; thin films

Introduction

With the advance of nanotechnology, the interest in the production of ultrathin polymer films as coatings or functional thin films increases too. Production of thin polymer films can be difficult. In the case of spin-coating, an imbalance between the surface tension, viscosity and the solvent evaporation can cause ultra thin films to break and holes to appear. Vacuum deposition generally cannot be used for polymers because they do not evaporate very easily and the high temperatures for vaporization will decompose the polymer in most cases.

In this paper, another means to prepare thin polymer films, electrospray deposition will be discussed. Electrospray, or electrohydrodynamic atomization, is the acceleration of a liquid under the influence of an electric field.[1] The liquid forms a jet, which breaks up into small droplets. Many spray modes exist in electrospray and one of the most stable and controllable is the cone-jet mode, which in general produces droplets with a narrow size distribution.[2,3] The cone jet mode has been thoroughly studied and theoretical descriptions of the jet formation and the droplet size have been obtained for this mode.[4–7]

The advantages of electrospray deposition for film preparation are that it can be used at room temperature and can be applied locally, in principle, in situ. The latter means that the film does not need to be lifted, a procedure that leads to additional risk of tearing of ultrathin films. Although electrospray deposition is not new, applications in thin film preparation are not widespread, because it is relatively unexplored as an ultrathin film preparation tool, especially where its use with polymers is concerned.[8–12] In this paper, it will be demonstrated that thin polymer film morphologies obtained with electrospray deposition can be controlled with an electrospray model. The polymer used in this paper is poly(vinylidene fluoride) (PVDF) and DMF was used as solvent

[1] Department of Electronic Science and Engineering, Kyoto University, A1-326, Katsura, Nishikyo-ku, Kyoto 615-8510, Japan
E-mail: rietveld@piezo.kuee.kyoto-u.ac.jp
[2] International Innovation Center, Kyoto University, Katsura, Nishikyo-ku, Kyoto 615-8520, Japan

for the spray. One important factor, the substrate, is ignored in this study, because the objective is to elucidate specifically the role of electrospray. In future research, the properties of the substrate will be incorporated into the approach.

Experimental Part

All experimental details are given elsewhere.[10,13] PVDF, 534,000 g/mol, and DMF were used as purchased. Polymer solutions were at least given 1 day to dissolve. Spray deposition took place in a nitrogen atmosphere, with a 6 L/min nitrogen gas flow during the experiments to flush solvent vapor out of the chamber. The temperature during spray deposition was 40 °C; for one sample series, the temperature was 20 °C. Films were collected on silicon wafer containing only a native layer of SiO_2.

The spray setup consists of a nozzle with a ring around the nozzle at the tip to stabilize the electrospray.[10] The ring had a potential of 3 kV in most experiments and the nozzle potential was in the order of 5 kV; for one sample series, the ring was 8 kV and the nozzle 9.2 kV. The current between the nozzle and the substrate was monitored during spraying. The distance between the nozzle and the substrate can be varied from 0 up to 12 cm. The substrate position was fixed during the spray deposition.

The films were analyzed with AFM and roughness averages of the films were determined as described in reference[10]. Matlab 7.2 version R2006a was used for the model calculations, the code of which can be found in reference[13].

Model

The model describes electrospray deposition in the cone-jet mode and provides the state of the droplet at deposition. A detailed description of the model can be found elsewhere.[13] Electrospray deposition consists of droplet generation, droplet evaporation, and deposition on the substrate. The initial droplet diameter, d, generated in the cone-jet mode can be calculated with:[7]

$$d = a\left(\frac{\rho\varepsilon_0 Q^4}{I^2}\right)^{1/6} \quad (1)$$

a is a calibration constant, which in the case of DMF is 1.5,[13] ρ is the density of the liquid, ε_0 is the dielectric constant of the liquid, Q the flow rate and I the current of the spray (all in SI units). Droplet evolution is calculated numerically using a general relationship for droplet evaporation[14] and the velocity of the evaporating droplet is obtained by calculating the balance between the electric force and the drag force.[13] The electric field between the nozzle and the substrate exerts a force on the droplets, because the droplets carry a small charge.[15] The current, I, in Equation 1 is also the result of this charge. With these basic elements, the size of the droplet, the velocity of the droplet, and the force on the droplet at impact can be calculated and these conditions can be correlated with a resulting film morphology.[10,13]

It is important to keep in mind that the model is constructed in such a way that it presents the state of the droplet at impact as a function of spray distance. This means that depicted trajectories as a function of the spray distance do not occur in real time; however, the points on the trajectories can be directly compared with experimentally imaged film morphologies as a function of the spray distance. The difference with real time is caused by the electric field, which changes when the distance between the nozzle and the substrate increases, affecting the droplet velocity.

Morphology Mapping

Spraying polymer solution results in different polymer morphologies depending on the conditions. Important factors are for example the initial polymer concentration in the droplet, the initial droplet size, the distance from the nozzle to the substrate, the temperature and the velocity of the

droplet. Another important factor is the properties of the solvent itself.[10]

As a function of spray distance, different morphologies have been observed with AFM (Figure 1). These morphologies include almost empty substrate, because excess solvent removed the deposited polymer (Figure 1a), a continuous film consisting of polymer blobs (Figure 1b) and a continuous film, which first becomes smoother with spray distance (Figure 1c and d) to become rougher again, when the droplet/polymer particle becomes drier (Figure 1e). Films produced with completely dry particles have not been shown here, because such films are too loose to provide clear AFM images.

From Figure 1, it can be concluded that an important factor in film formation is the presence of solvent depositing together with polymer; it is however not the complete explanation, as will be shown below. Not only the spray distance gives rise to this morphology sequence, but also the temperature and the droplet size, for example. To study the morphology as a function of a number of conditions, a morphology is required, which can be determined accurately. The continuous films in Figure 1c, d and e exhibit a clear change in the roughness average going through a minimum. Roughness can be conveniently quantified as the average deviation of the average height in an AFM image. The roughness minimum is therefore an excellent marker to study the effect of changing conditions on the morphology.

The roughness average parameter depends on the size of the AFM image, therefore only roughness parameters of the same image size can be compared with each other. Furthermore, film thickness is an important factor influencing film roughness. In general, the roughness increases with increasing film thickness until the roughness average levels off (Figure 2). In the case of electrosprayed PVDF on AFM images of 25×25 μm, the saturation thickness is 300 nm. To avoid the effect of thickness fluctuations in the comparison of the roughness average under different conditions, a film thickness of 400 nm was used.

In Figure 3, roughness average values are shown of several films made with different droplet sizes (Table 1, for clarity not all droplet sizes have been plotted in Figure 3) and one film made with a different initial concentration. For all droplet sizes, the roughness average shows a clear minimum as a function of spray distance. It can be seen that the position of the minima is affected by the droplet size, but not by the concentration.

Since film morphology is not determined by the initial droplet, but by the droplet which impinges on the surface, the droplet evolution model was used to determine the droplet size as a function of distance from the nozzle to the substrate. The size decrease for the five cases given in Table 1 is presented in Figure 4. The spray distance with minimum roughness has been marked with diamonds. From this figure, it is clear that not only the amount of solvent

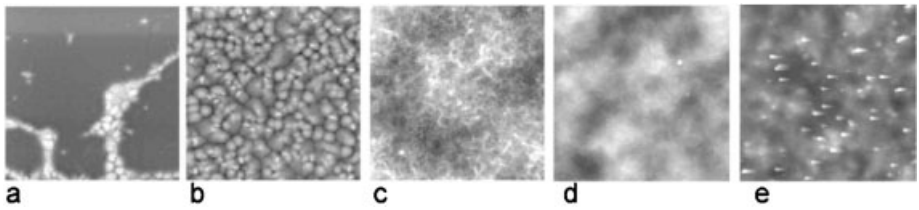

Figure 1.
A number of morphologies of PVDF on Si-wafer as a function of spray distance. Spray conditions PVDF in DMF 0.5 wt%, flow rate 3 μl/min, current 24 nA, spray distance a) 1 cm, b) 1.5 cm, c) 2 cm, d) 2.25 cm, e) 4 cm. The size of the images is 25 μm × 25 μm.

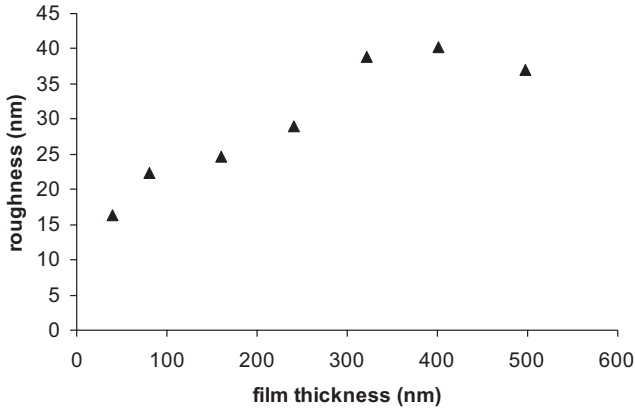

Figure 2.
Roughness average as a function of film thickness. Roughness average values were determined of films with a morphology similar to the one in Figure 1d. 25μm images were used. Spray conditions: PVDF in DMF 1 wt%, flow rate 3 μl/min, spray distance 3 cm, current 25 nA and stepwise increased spray times.

is responsible for the formation of smooth film. An indication was already present in Figure 3, because an increase in the polymer concentration does not alter the spray distance, where the minimum roughness occurs. The concentration only changes the value of the roughness. In Figure 4, it can be seen that the smaller the droplet, the more it evaporates relatively before the film with minimum roughness forms. All droplets have the same initial concentration in Figure 4, therefore the polymer concentration in the droplets is different at the marked impact distance. This excludes the concentration as a main determining factor of film morphology.

Then what determines the relation between the minimum roughness and the necessary solvent in the impinging droplets? The explanation follows from the observation that electrospray forms a cone of droplets, which increases with the spray distance. The increase of the droplet cone can be determined by measuring the surface covered by film for a number of spray distances. The obtained relationship is:

$$r = 4.8x^2 + 0.15x \tag{2}$$

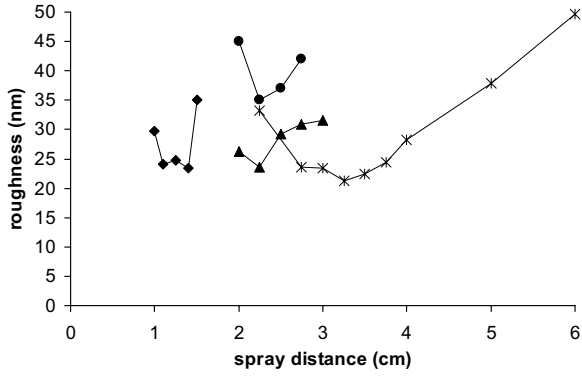

Figure 3.
Roughness average as a function of spray distance for different droplet diameters (Table 1, row 1, 3 and 5). PVDF in DMF 0.25 wt%: diamonds 1.7 μm, triangles 3.4 μm, asterisks 5.0 μm. 1 wt%: circles 3.4 μm. Lines are a guide for the eye. In all cases, the roughness average was determined with AFM images of 25 μm.

Table 1.
Spray conditions and resulting droplet diameters (Equation 1).

Q (μl/min)	I (nA)	d (μm)
1.2	27	1.7
2.5	50	2.3
3.0	21	3.4
4.0	25	3.9
6.0	26	5.0

with r the radius of the film produced with electrospray and x the distance between the nozzle and the substrate in meter.

The increase of deposition area, suggests a relationship between the film morphology and the droplet size in combination with the available space on the surface (Figure 5). If the locations of the minimum roughness values are plotted in Figure 5, a straight line results, intersecting the abscissas at zero. The graph represents the change in the surface and time interval that a droplet has available to spread, before another droplet deposits in the same area. The value of the x-axis is obtained from the spray distance, by calculating the size of the deposit with Equation 2 and dividing it by the number of droplets generated per second by electrospray (the flow divided by the volume of the droplets). The straight line, fitting the measured minimum roughness locations, represents the conditions for the minimum roughness. The line does not predict how smooth the film is, but it predicts that the morphology is the smoothest continuous film for a particular set of conditions. This demonstrates that the spreading conditions of the impinging droplets determine the morphology of the film. Another way to view the straight line is to consider it as a growth rate of material -polymer and solvent- depositing on the available surface. Depending on the growth rate, a specific morphology will form; for the minimum roughness the growth rate is 0.20 μm/s. Similar analyses can be done for the other morphologies presented in Figure 1, but here the focus will be on the minimum roughness to show the capability to predict a morphology depending on the spray conditions.

Morphology Prediction

To demonstrate that this approach can predict the minimum roughness under different electrospray conditions, three cases will be presented, summarized in Table 2. In the first example, the spray conditions are the same as for the films from which the relationship has been derived (Table 1), but the films are only 50 nm thick instead of 400 nm. In Figure 6, a similar graph as the one in Figure 5 is presented with the evaporation trajectory of the example conditions. The dash-dot line represents the droplet evaporation of the 50 nm thick films. The conditions under which the smoothest film occurs, the

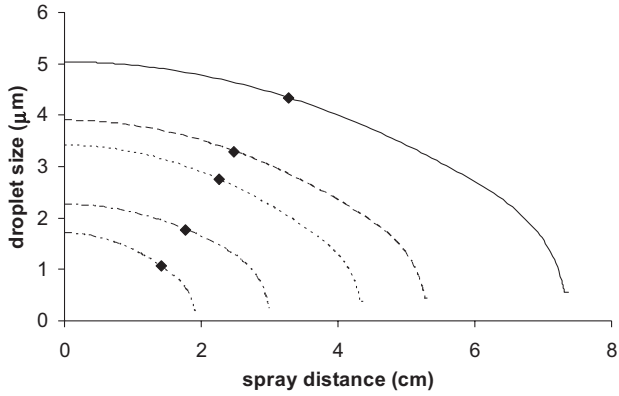

Figure 4.
Evaporation curves of the droplet sizes from Table 1. The diamonds on the curve are the spray distances, where the film with the lowest roughness forms (Figure 3).

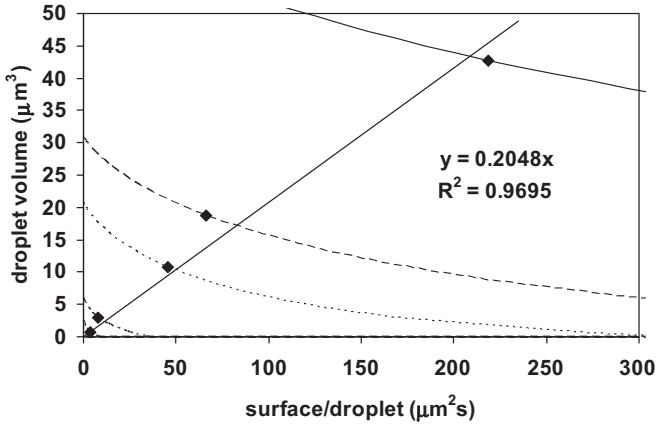

Figure 5.
Droplet evaporation plotted as the droplet volume against the available surface per droplet on the substrate. The curves are the evaporation trajectories of the respective droplet sizes, given in Table 1. The diamonds are the locations of minimum roughness. The straight line is a linear fit through the data representing the conditions for the minimum roughness.

straight line, crosses the evaporation trajectory at 58, which translates into a spray distance of 2.4 cm (Table 2) with Equations 1 and 2.

In Figure 7, the experimental roughness average values are presented of two 50 nm thick films, one made with a concentration of 0.1 wt% PVDF in DMF and the other made with 0.025 wt%. The prediction of the spray distance where the smoothest film occurs coincides with the experimentally determined location. Moreover, also in this case the lowest concentration provides the lowest roughness average.

In the next example, the velocity of the droplet is higher. The droplet size at deposition depends on the evaporation rate, but also on the velocity of the droplet between the nozzle and the substrate for a given nozzle-substrate distance; a detailed description of the dependence can be found in reference [13]. Since droplets generated with electrospray are charged, an increase in the electric field will increase the velocity of the droplets. However to ensure a stable cone-jet mode, the electric field at the tip of the nozzle must be within a specific range. The necessary electric field depends on the properties of the sprayed liquid.[6,16] To allow the increase of the electric field between the nozzle and the substrate without affecting the cone-jet mode, a ring is placed at the tip of the nozzle. During most of the experiments, the ring has a voltage of 3 kV, but in the following example, the ring is 8 kV, forcing the nozzle to be approximately 9.2 kV to maintain a cone-jet mode. However, because the droplets move faster, the droplet cone is narrower, so Equation 2 needs to be recalibrated (r and x in meter):

$$r_{8000\,\mathrm{kV}} = 1.2x^2 + 0.14x - 0.001 \qquad (3)$$

The calculated droplet evaporation trajectory is shown in Figure 6. The intersec-

Table 2.
Predictions of the spray distance of minimum film roughness under different spray conditions of PVDF in DMF at 40 °C and with the potential of the ring at the tip of the nozzle 3 kV (unless indicated otherwise).

Sample description	Q (μl/min)	I (nA)	Prediction (cm)	Measured (cm)
Films ~50 nm thick	3	19	2.4	2.4–2.5
Ring 8 kV	3	23	3.7	3.8
20 °C	2	70	2.1	2.0–2.5

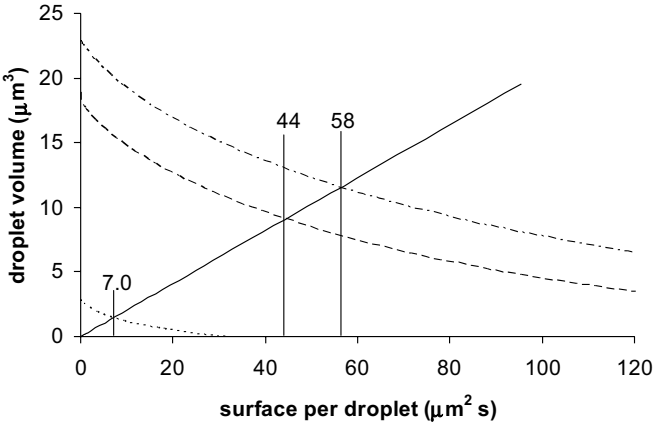

Figure 6.
Droplet evaporation trajectories under different spray conditions (Table 2). Dash dotted line: 50 nm thick films, dashed line: 8 kV, dotted line: 20 °C. The numbers in the graph refer to the surface area available for the droplet, at the conditions for smoothest film.

tion with the prediction for the smoothest film is found at 44, which is equal to 3.7 cm using Equation 1 and 3 and the data from Table 2. This is the same as found with the experimental data (Figure 7 and Table 2).

All the previous examples were films prepared at 40 °C. In the following example, the samples were prepared at 20 °C; other conditions are given in Table 2. The dotted line in Figure 6 presents the evaporation trajectory of the droplets sprayed at 20 °C. Using Equation 1 and 2, the intersection at 7.0 corresponds to 2.1 cm. Although 2.1 cm does not necessarily differ from the experimental data (Figure 7, filled diamonds), the fit appears to be less good than the previous two examples. Part of the explanation is most likely that temperature influences the spray deposition in many different ways, which is not

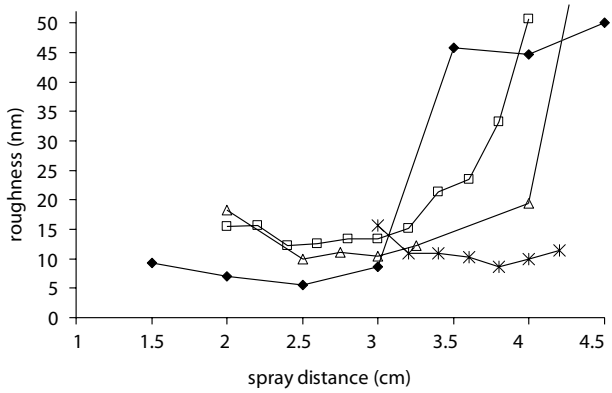

Figure 7.
Plot of roughness average values versus spray distance of films prepared under different conditions (Table 2). 1) 50 nm thick films prepared with 0.1 wt% (open squares) and 0.025 wt% (open triangles). 2) Ring potential at the tip of the nozzle 8 kV and concentration 0.05 wt% (asterisk). Roughness average in case 1 and 2 determined with 25 μm AFM images. 3) Films prepared at 20 °C with 0.05 wt% (filled diamonds). Roughness average determined with 5 μm AFM images. The jump in roughness between 3 and 4 cm is caused by a fast increase of evaporation due to a small droplet size (<1 μm).

completely accounted for in the model. One important effect, but not the only one, is the fact that solvent, depositing with the polymer, still evaporates from the film, while droplet deposition continues. This is partly incorporated, because the values of the x-axis consist of 'surface and time interval per droplet' (μm^2s/droplet), indicating that the volume of the droplet is plotted against a time for the droplet to evaporate and a surface to spread. This means that the evaporation of the solvent is incorporated as long as the temperature remains the same. With a decrease in temperature, the solvent will evaporate more slowly from the surface and therefore the roughness minimum is expected to shift to higher surface-time per droplet, which is what is observed in the last example. One could compensate for this by fully incorporating the solvent evaporation from the surface; however, because films are highly concentrated solutions of solvent dissolved in a matrix of polymer, the evaporation cannot be approximated with that of the pure solvent. In addition, the precise interaction parameters of the solvent with the polymers might not be known, which makes the calculation of the evaporation rate of the solvent difficult. It may be necessary to decouple the surface and time element in the x-axis of Figure 5 and 6 experimentally. This can be done by scanning the sample during spray deposition, which allows the spray distance and deposition time, related with the scan movement, to be controlled separately.

Conclusion

PVDF film morphology with electrospray deposition depends on three factors, the volume of the droplet at impact, the substrate surface available per droplet and the solvent evaporation rate from the film. The employment of the model describing droplet size and droplet evaporation makes it possible to reduce a large number of parameters to these three factors, which can be summarized in a growth rate. Once the growth rate for a specific morphology is known, the occurrence of the morphology under different conditions can be predicted.

Acknowledgements: This work was supported by the Integrated Industry Academia Partnership (IIAP), Kyoto University International Innovation Center.

[1] G. Taylor, *Proc. R. Soc. London, A* **1964**, *A280*, 383.
[2] M. Cloupeau, B. Prunet-Foch, *J. Electrostatics* **1989**, *22*, 135.
[3] J. M. Grace, J. C. M. Marijnissen, *J. Aerosol Sci.* **1994**, *25*, 1005.
[4] A. M. Ganan-Calvo, *Phys. Rev. Lett.* **1997**, *79*, 217.
[5] A. M. Ganan-Calvo, J. Davila, A. Barrero, *J. Aerosol Sci.* **1997**, *28*, 249.
[6] R. P. A. Hartman, D. J. Brunner, D. M. A. Camelot, J. C. M. Marijnissen, B. Scarlett, *J. Aerosol Sci.* **1999**, *30*, 823.
[7] R. P. A. Hartman, D. J. Brunner, D. M. A. Camelot, J. C. M. Marijnissen, B. Scarlett, *J. Aerosol Sci.* **2000**, *31*, 65.
[8] C. Berkland, D. W. Pack, K. Kim, *Biomaterials* **2004**, *25*, 5649.
[9] N. Fujitsuka, J. Sakata, Y. Miyachi, K. Mizuno, K. Ohtsuka, Y. Taga, O. Tabata, *Sens. Actuators, A* **1998**, *A66*, 237.
[10] I. B. Rietveld, K. Kobayashi, H. Yamada, K. Matsushige, *J. Colloid Interface Sci.* **2006**, *298*, 639.
[11] R. Saf, M. Goriup, T. Steindl, T. E. Hamedinger, D. Sandholzer, G. Hayn, *Nat. Mater.* **2004**, *3*, 323.
[12] J. Sakata, M. Mochizuki, *Thin Solid Films* **1991**, *195*, 175.
[13] I. B. Rietveld, K. Kobayashi, H. Yamada, K. Matsushige, *J. Phys. Chem. B* **2006**, *110*, 23351.
[14] W. C. Hinds, "*Aerosol Technology, Properties, Behavior, and Measurement of Airborne Particles*", John Wiley & Sons, Inc., New York 1998, p. 286.
[15] P. Kebarle, Y. Ho, in: "*Electrospray Ionization Mass Spectrometry*", 1st ed.,R. B. Cole, Ed., John Wiley & Sons, New York 1997, p. 3.
[16] A. M. Ganan-Calvo, *J. Fluid Mech.* **1997**, *335*, 165.

